Inorganic Chemistry

ARTICLE

pubs.acs.org/IC

Dinuclear Cobalt(II) and Copper(II) Complexes with a $Py_2N_4S_2$ Macrocyclic Ligand

Cristina Núñez,[†] Rufina Bastida,[*,†] Luis Lezama,[‡] Alejandro Macías,[†] Paulo Pérez-Lourido,[§] and Laura Valencia[*,§]

[†]Departamento de Química Inorgánica, Facultade de Química, Universidade de Santiago de Compostela, Avenida das Ciencias s/, E-15782 Santiago de Compostela, La Coruña, Spain

[‡]Departamento de Química Inorgánica, Facultad de Ciencia y Tecnología, Universidad del Pais Vasco/EHU, Apartado 644, 48080 Bilbao, Spain

[§]Departamento de Química Inorgánica, Universidade de Vigo, Lagoas-Marcosende /n, 36310 Vigo, Pontevedra, Spain

ABSTRACT:

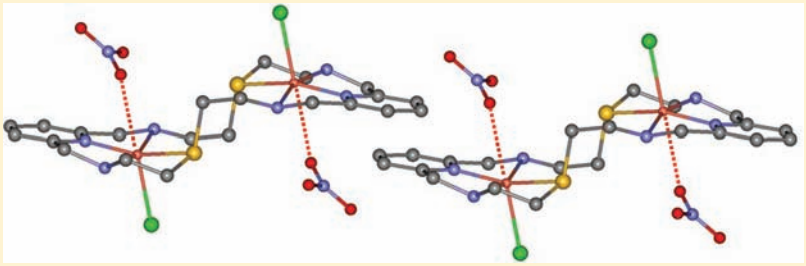

The interaction between Co^{II} and Cu^{II} ions with a $Py_2N_4S_2$-coordinating octadentate macrocyclic ligand (L) to afford dinuclear compounds has been investigated. The complexes were characterized by microanalysis, conductivity measurements, IR spectroscopy and liquid secondary ion mass spectrometry. The crystal structure of the compounds $[H_4L](NO_3)_4$, $[Cu_2LCl_2](NO_3)_2$ (**5**), $[Cu_2L(NO_3)_2](NO_3)_2$ (**6**), and $[Cu_2L(\mu\text{-}OH)](ClO_4)_3\cdot H_2O$ (**7**) was also determined by single-crystal X-ray diffraction. The $[H_4L]^{4+}$ cation crystal structure presents two different conformations, planar and step, with intermolecular face-to-face π,π-stacking interactions between the pyridinic rings. Complexes **5** and **6** show the metal ions in a slightly distorted square-pyramidal coordination geometry. In the case of complex **7**, the crystal structure presents the two metal ions joined by a μ-hydroxo bridge and the Cu^{II} centers in a slightly distorted square plane or a tetragonally distorted octahedral geometry, taking into account weak interactions in axial positions. Electron paramagnetic resonance spectroscopy is in accordance with the dinuclear nature of the complexes, with an octahedral environment for the cobalt(II) compounds and square-pyramidal or tetragonally elongated octahedral geometries for the copper(II) compounds. The magnetic behavior is consistent with the existence of antiferromagnetic interactions between the ions for cobalt(II) and copper(II) complexes, while for the Co^{II} ones, this behavior could also be explained by spin−orbit coupling.

INTRODUCTION

The design of ligands capable of forming dinuclear cobalt(II) and copper(II) complexes has attracted increasing attention in recent years,[1−3] with their functional role in many metalloenzymes being one of the main research focuses.[4] For this reason, the synthesis of complexes aimed at mimicking the metal sites of different types of metalloproteins constitutes an important branch in both inorganic and organic chemistry.

Proteins containing copper ions at their active site are usually involved as redox catalysts in a wide range of biological processes. Type 3 active-site copper-containing proteins present a dicopper core in which both metal ions are surrounded by three nitrogen donor atoms from histidine residues.[5] They are able to reversibly bind dioxygen at ambient conditions. The Cu^{II} ions in the oxy state of these proteins are strongly antiferromagnetically coupled, leading to electron paramagnetic resonance (EPR)-silent behavior. This class of enzymes is represented by three proteins, namely, tyrosinase, hemocyanin, and catechol oxidase.

From various chemical and spectroscopic studies,[6] it is known that tyrosinase contains a coupled dinuclear copper site with histidine ligation similar to that of hemocyanin, the structure of which is known.[7] Preliminary data regarding the structure of the catechol oxidase from sweet potatoes (*Ipomoea batatas*) have been reported.[8] This enzyme also contains a coupled dinuclear copper site, with three histidine ligands per copper atom and an additional hydroxide bridge in the oxidized form, but unlike tyrosinase, it is only active in the transformation of *o*-diphenol to *o*-quinones and not in the hydroxylation of phenols to diphenols.

Received: February 10, 2011
Published: May 25, 2011

Scheme 1

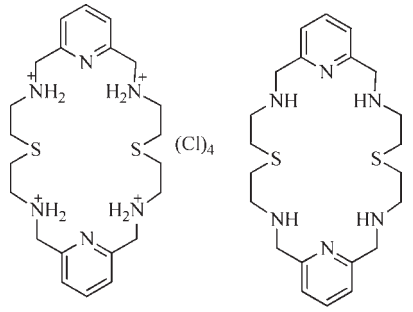

$[H_4L]Cl_4$ L

Several metalloproteins containing cobalt coordinated to histidine, aspartic, and glutamic acids, such as methionine aminopeptidase, prolidase, glucose isomerase, methylmalonyl-CoA carboxytransferase, lysine 2,3-aminomutase, and aldehyde decarboxylase, were also characterized.[9] Cobalt has also been used to replace other metal ions present in metalloproteins because of its high sensitivity to the coordination site geometry, which means that information can be gathered about changes of the metal sites in proteins during protein function.[10]

On the other hand, macrocyclic ligands incorporating nitrogen and sulfur in their framework are not as numerous as those with nitrogen and oxygen, and reviews including macrocycles with sulfur are not common in the literature.[11]

Therefore, as part of our research in the field of transition-metal complexes with different macrocyclic ligands, here we report the synthesis, characterization, and study of cobalt(II) and copper(II) nitrate and perchlorate complexes with the potential octadentate sulfur- and nitrogen-containing macrocyclic ligand $Py_2N_4S_2$ (**L**), which has the capability of forming dinuclear complexes (Scheme 1).[12]

EXPERIMENTAL SECTION

Chemicals and Starting Materials. The synthesis of **L** was achieved following the literature method.[13] 2,6-Pyridinedimethanol, 1,5-diamine-3-tiopenthane, and hydrated nitrate and perchlorate salts were commercial products (ABCR or Aldrich). The solvents used were of reagent grade and were purified by the usual methods.

Caution! *Although problems were not encountered during the course of this work, attention is drawn to the potentially explosive nature of perchlorate salts.*

Measurements. Elemental analyses were performed on a Fisons Instruments EA1108, and IR spectra were recorded as KBr disks on a Bio-Rad FTS 175-C spectrometer. Liquid secondary ion mass spectrometry (LSI-MS) were recorded using a Kratos MS50TC spectrometer with 3-nitrobenzyl alcohol as the matrix. Conductivity measurements were carried out in 10^{-3} mol dm^{-3} acetonitrile solutions at 20 °C using a WTW LF3 conductivimeter. X-band EPR measurements were carried out on a Bruker ELEXSYS 500 spectrometer equipped with a superhigh-Q resonator ER-4123-SHQ and standard Oxford Instruments low-temperature devices. The spectra were recorded using a typical modulation amplitude of 0.1 mT at a frequency of 100 kHz. For Q-band studies, EPR spectra were recorded on a Bruker EMX system equipped with an ER-510-QT resonator and an ER-4112-HV liquid-helium cryostat. The magnetic field was calibrated with an NMR probe, and the frequency inside the cavity was determined with a Hewlett-Packard 5352B microwave-frequency counter. Magnetic susceptibility measurements were performed on powdered samples between 1.8 and 300 K with a Quantum Design MPMS-7 Squid magnetometer. The magnetic field used in the experiments was 0.1 T, a value at which the magnetization versus magnetic field curve was still linear at 1.8 K. Experimental susceptibility values were corrected for the diamagnetic contributions and for the temperature-independent paramagnetism.

Synthesis of L. The protonated ligand $[\mathbf{H_4L}]\mathbf{Cl_4}$ was isolated as an air-stable white solid in 61% yield by using a three-step procedure involving cyclocondensation of 2,6-diformylpyridine with 1,5-diamine-3-tiopenthane followed by an in situ reaction with $NaBH_4$ and subsequent treatment with HCl. The macrocyclic ligand **L** was isolated as an air-stable yellow oil in 49% yield after dissolution of the ligand $[\mathbf{H_4L}]\mathbf{Cl_4}$ in H_2O and adjustment of the pH to 11 with NaOH.

Synthesis of the Metal Complexes. *General Procedure.* A solution of the appropriate metal salt (0.08 mmol) in ethanol (5 mL) was added dropwise to a stirred solution of the ligand **L** (0.04 mmol), in the same solvent (25 mL). In all cases, the appearance of a precipitate was observed immediately after the addition of the metal salt. The solution was softly heated at 40 °C and stirred for 4 h. The precipitate formed was isolated by centrifugation and dried under vacuum, yielding the metal complexes of the ligand.

In a similar procedure, a solution of hydrated nickel(II) or copper(II) nitrate (0.08 mmol) in ethanol (5 mL) was added dropwise to a stirred solution of the ligand $[\mathbf{H_4L}]\mathbf{Cl_4}$ (0.04 mmol) in the same solvent (25 mL). Slow evaporation of the ethanolic solution yielded crystals of $[H_4L](NO_3)_4$ and $[Cu_2LCl_2](NO_3)_2$ (**5**), respectively.

*$[Co_2L](NO_3)_4 \cdot 2H_2O$ (**1**).* Anal. Calcd for $C_{22}H_{38}N_{10}O_{14}S_2Co_2$ (MW: 847.8): C, 31.1; H, 4.4; N, 16.5; S, 7.5. Found: C, 31.3; H, 4.2; N, 16.1; S, 7.5. Yield: 55%. IR (KBr, cm^{-1}): 1606, 1471 [ν(C=N)$_{py}$ and ν(C=C)], 1384, 1300 [$\nu(NO_3^-)$]. LSI-MS (m/z): 505 [CoL]$^+$, 447 [L + H]$^+$. Conductivity (μS cm^{-1}, in CH_3CN, 1×10^{-3} M): 265 (2:1). Color: brown.

*$[Co_2L](ClO_4)_4 \cdot C_2H_6O$ (**2**).* Anal. Calcd for $C_{24}H_{40}N_6O_{17}S_2Cl_4Co_2$ (MW: 1007.8): C, 28.5; H, 3.9; N, 8.3; S, 6.4. Found: C, 28.1; H, 3.9; N, 8.6; S, 6.6. Yield: 43%. IR (KBr, cm^{-1}): 1606, 1454 [ν(C=N)$_{py}$ and ν(C=C)], 1109, 627 [$\nu(ClO_4^-)$]. LSI-MS (m/z): 505 [CoL]$^+$, 447 [L + H]$^+$. Conductivity (μS cm^{-1}, in CH_3CN, 1×10^{-3} M): 298 (2:1). Color: brown.

*$[Cu_2L](NO_3)_4 \cdot 2H_2O$ (**3**).* Anal. Calcd for $C_{22}H_{38}N_{10}O_{14}S_2Cu_2$ (MW: 857.08): C, 30.8; H, 4.4; N, 16.3; S, 7.4. Found: C, 30.3; H, 4.6; N, 16.1; S, 7.2. Yield: 76%. IR (KBr, cm^{-1}): 1607, 1475 [ν(C=N)$_{py}$ and ν(C=C)], 1383, 1300 [$\nu(NO_3^-)$]. LSI-MS (m/z): 760 $[Cu_2L(NO_3)_3]^+$, 697 $[Cu_2L(NO_3)_2]^+$, 635 $[Cu_2L(NO_3)]^+$, 509 [CuL]$^+$, 509 [CuL]$^+$, 447 [L + H]$^+$. Conductivity (μS cm^{-1}, in CH_3CN, 1×10^{-3} M): 273 (2:1). Color: blue.

*$[Cu_2L](ClO_4)_4$ (**4**).* Anal. Calcd for $C_{22}H_{34}N_6O_{16}S_2Cl_4Cu_2$ (MW: 971.08): C, 27.2; H, 3.5; N, 8.7; S, 6.6. Found: C, 28.0; H, 3.6; N, 8.7; S, 6.9. Yield: 71%. IR (KBr, cm^{-1}): 1606, 1454 [ν(C=N)$_{py}$ and ν(C=C)], 1109, 627 [$\nu(ClO_4^-)$]. LSI-MS (m/z): 709 $[CuL(ClO_4)_2]^+$, 509 [CuL]$^+$, 447 [L + H]$^+$. Conductivity (μS cm^{-1}, in CH_3CN, 1×10^{-3} M): 246 (2:1). Color: blue.

X-ray Crystallography. Measurements were made on a Bruker SMART CCD 1000 area diffractometer. All data were corrected for Lorentz and polarization effects. Empirical absorption corrections were also applied to all of the crystal structures obtained.[14] Complex scattering factors were taken from the program package *SHELXTL*.[15] The structures were solved by direct methods, which revealed the positions of all non-hydrogen atoms. All of the structures were refined on F^2 by a full-matrix least-squares procedure using anisotropic displacement parameters for all non-hydrogen atoms. The hydrogen atoms were located in their calculated positions and refined using a riding model. Molecular graphics were obtained with *ORTEP-3*.[16]

dx.doi.org/10.1021/ic200287f |*Inorg. Chem.* 2011, 50, 5596–5604

Table 1. Crystal Data and Structure Refinement for $[H_4L](NO_3)_4$ and 5−7

	$[H_4L](NO_3)_4$	$[Cu_2LCl_2](NO_3)_2$	$[Cu_2L(NO_3)_2](NO_3)_2$	$[Cu_2L(\mu\text{-}OH)](ClO_4)_3\cdot H_2O$
empirical formula	$C_{22}H_{38}N_{10}O_{12}S_2$	$C_{22}H_{34}N_8O_6Cl_2Cu_2S_2$	$C_{22}H_{34}N_{10}O_{12}Cu_2S_2$	$C_{22}H_{37}N_6O_{14}Cu_2Cl_3S_2$
fw	698.74	768.67	821.79	907.13
T (K)	293(2)	293(2)	293(2)	293(2)
wavelength (Å)	0.710 73	0.710 73	0.710 73	0.710 73
cryst syst	triclinic	triclinic	triclinic	triclinic
space group	$P\bar{1}$	$P\bar{1}$	$P\bar{1}$	$P\bar{1}$
a (Å)	8.2735(3)	7.5579(10)	7.7107(3)	9.2943(6)
b (Å)	12.9362(5)	7.7847(12)	8.3294(4)	11.1393(6)
c (Å)	15.5582(7)	12.925(2)	12.5934	17.2770(10)
α (deg)	97.979(2)	103.345(11)	100.855(3)	77.604(5)
β (deg)	104.608(2)	99.189(11)	98.072(3)	84.509(4)
γ (deg)	104.005(2)	103.414(7)	107.062(2)	70.161(4)
V (Å^3)	1527.61(11)	701.21(19)	742.71(6)	1642.83(17)
Z	2	1	1	2
calcd density (g cm^{-3})	1.519	1.820	1.837	1.834
abs coeff (mm^{-1})	0.252	1.912	1.654	1.742
F(000)	736	394	422	928
cryst size (mm)	0.58 × 0.26 × 0.04	0.17 × 0.16 × 0.01	0.13 × 0.04 × 0.02	0.21 × 0.08 × 0.03
θ range (deg)	1.38−28.32	1.66−26.34	1.68−26.02	1.21−26.37
reflns collected	67 080	7369	14 118	18 745
indep reflns (R_{int})	7456 (0.1027)	2838 (0.0784)	2922 (0.0495)	6671 (0.0567)
completeness (%) to θ (deg)	98.0 (28.23)	99.1 (26.34)	99.9 (26.02)	99.4 (26.37)
abs corrn	SADABS	SADABS	SADABS	SADABS
max and min transmn	0.9900 and 0.8675	0.9811 and 0.7370	0.9677 and 0.8137	0.949 and 0.8137
data/restraints/param	7456/0/415	2838/6/190	2922/6/225	6671/0/454
GOF on F^2	1.024	1.057	1.066	1.022
final R indices [$I > 2\sigma(I)$]	R1 = 0.0488, wR2 = 0.1282	R1 = 0.0898, wR2 = 0.2342	R1 = 0.0469, wR2 = 0.1232	R1 = 0.0625, wR2 = 0.1608
R indices (all data)	R1 = 0.0760, wR2 = 0.1436	R1 = 0.1441, wR2 = 0.2545	R1 = 0.0627, wR2 = 0.1316	R1 = 0.1032, wR2 = 0.1759
$\Delta\rho_{max}$ and $\Delta\rho_{min}$ (e Å^{-3})	1.567 and −0.429	1.787 and −1.318	0.913 and −0.784	1.150 and −0.746

RESULTS AND DISCUSSION

Synthesis and General Characterization. The coordination ability of ligand **L** toward hydrated nitrate and perchlorate salts of cobalt(II) and copper(II) was studied. The reaction of **L** with the appropriate hydrated metal salt in a 2:1 metal-to-ligand molar ratio in ethanol led to dinuclear complexes in good yield (43−76%). The ligand reacted quickly with Co^{II} and Cu^{II} ions, producing air-stable solids soluble in water and acetonitrile and insoluble in other solvents. They were characterized by elemental analysis, IR, LSI-MS, and conductivity measurements.

The IR spectra of the complexes were recorded as KBr disks, and they all showed similar features. The bands due to the ν(C═N) and ν(C═C) stretching modes of the pyridine rings are generally shifted to higher wavenumbers when compared to their positions in the spectrum of the free ligand, suggesting coordination of the pyridyl groups to the metal ions.[17] The spectra of nitrate complexes show an intense band at 1380 cm^{-1} with a shoulder at ca. 1300 cm^{-1}, suggesting the presence of both coordinate and ionic nitrate groups.[18] The perchlorate complexes feature absorptions attributable to ionic perchlorate at 1100 and 625 cm^{-1}, indicating that these groups are not coordinated to the metal centers.[19]

The LSI mass spectra indicate evidence of the formation of the complexes. The peaks corresponding to fragments with the general formulas $[M_2LX_3]^+$, $[M_2LX_2]^+$, $[M_2LX]^+$, $[MLX_2]^+$, or $[ML]^+$ (M = Cu or Co; X = NO_3^- or ClO_4^-) are observed.

The molar conductivity values obtained at room temperature using acetonitrile as the solvent lie in the range previously observed for 2:1 electrolytes, in all cases.[20]

X-ray Diffraction. Crystals of $[H_4L](NO_3)_4$ and $[Cu_2LCl_2](NO_3)_2$ (**5**) suitable for X-ray diffraction were obtained by evaporation of an ethanolic solution of $[H_4L]Cl_4$ in the presence of nickel(II) and copper(II) nitrate, respectively. Slow evaporation from water solutions of **3** and **4** afforded single crystals of $[Cu_2L(NO_3)_2](NO_3)_2$ (**6**) and $[Cu_2L(\mu\text{-}OH)](ClO_4)_3\cdot H_2O$ (**7**), respectively. Details of the X-ray crystal data and structure solution and refinement for all crystal structures are given in Table 1.

Crystal Structure of $[H_4L](NO_3)_4$. The crystal structure of $[H_4L](NO_3)_4$ reveals the presence of the tetraprotonated ligand $[H_4L]^{4+}$ and four nitrate ions. The molecular structures of two different conformations, A and B, for the $[H_4L]^{4+}$ cation, together with selected bond lengths and angles, are given in Figure 1a.

In A, the aromatic rings are parallel and the planes containing these rings are only 1.33 Å apart, giving rise to an almost planar conformation. However, B shows a step conformation where the aromatic rings are also parallel, but in this case, the distance between the planes containing the aromatic rings is 3.45 Å. The protonated amine groups of the ligand establish different hydrogen-bond interactions with the free nitrate ions. All of these data are collected in Table 2. Additional intermolecular face-to-face π,π-stacking interactions have been found between the pyridinic

dx.doi.org/10.1021/ic200287f |*Inorg. Chem.* 2011, 50, 5596–5604

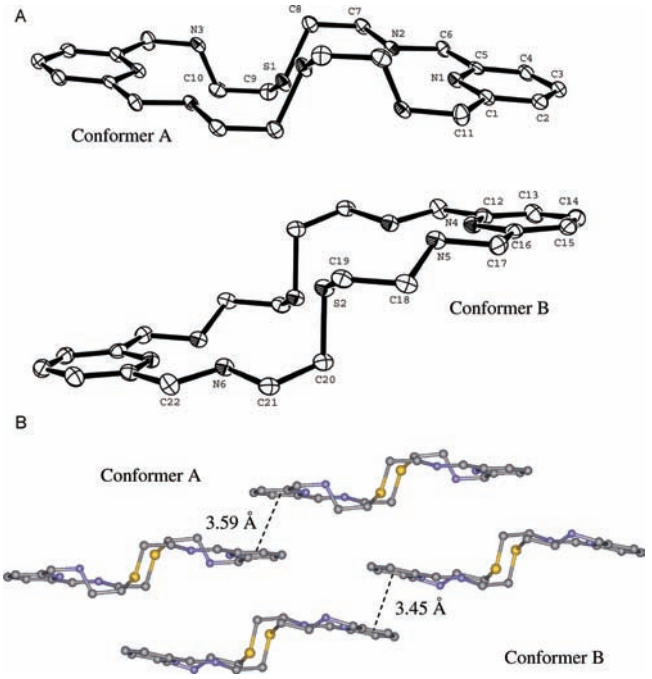

Figure 1. (a) Crystal structure of the $[H_4L]^{4+}$ conformers. Selected bond lengths (Å) and angles (deg): C1−N1 1.344(3), C5−N1 1.339(3), C7−N2 1.483(3), C8−S1 1.814(2), C9−S1 1.820(2), C10−N3 1.488(3), C12−N4 1.338(3), C16−N4 1.345(3), C17−N5 1.487(3), C18−N5 1.490(3), C19−S2 1.818(2), C20−S2 1.810(2), C21−N6 1.494(3), C22−N6 1.482(3); C7−N2−C6 111.99(15), C12−N4−C16 118.33(18), C17−N5−C18 116.50(16), C22−N6−C21 112.35(16), C8−S1−C9 101.73(10), C20−S2−C19 100.52(10). (b) π,π-Stacking interactions between the pyridine groups of adjacent molecules in conformers A and B of $[H_4L]^{4+}$.

rings of adjacent molecules, which give rise to infinite chains of each conformer (Figure 1b). The distances between centroids are 3.59 and 3.45 Å for conformers A and B, respectively.

Crystal Structure of ***5***. The crystal structure of $[Cu_2LCl_2](NO_3)_2$ (**5**) is consistent with that of the cationic complex $[Cu_2LCl_2]^{2+}$ and two nitrate ions. The molecular structure of **5** is shown in Figure 2a, along with the atom numbering scheme and selected bond lengths and angles. The macrocycle encloses two Cu^{II} ions, which are coordinated to a pyridinic nitrogen atom, one sulfur atom, two secondary amine groups from the macrocyclic backbone, and one chloride ion. The coordination geometry for the copper ions can be best described as a slightly distorted square pyramid (τ = 0.04). The Cu^{II} ions are displaced from the coordination plane [plane S1−N2−N1−N3; root mean square (rms) 0.0843] by 0.27 Å, while the apical position is occupied by the chloride ion. This chloride provides the longest bond to the copper ion, 2.506 Å, and the pyridinic nitrogen bond distance is shorter (1.940 Å) than the amine ones (2.027 and 2.077 Å). The sulfur bond distance is 2.374 Å, and the Cu---Cu distance is 5.792 Å. If we consider the long interaction established between an oxygen atom from a nitrate ion and the metal center, (Cu1−O2n 2.939 Å), the structure could also be described as distorted octahedral.

The ligand shows a step conformation with the planes containing the pyridinic rings at 2.74 Å. Intermolecular face-to-face π, π-stacking interactions between the pyridinic rings of adjacent molecules have been found (Figure 2b). The distance between the planes containing the aromatic rings is 3.12 Å, while the distance between centroids is 3.38 Å. In addition, different hydrogen-bond interactions have been observed between the free nitrate ions and the secondary amine groups of the ligand (see Table 2).

Table 2. Hydrogen-Bond Interactions for $[H_4L](NO_3)_4$ and 5−7

D−H···A[a]	distance (Å) H···A	D−H···A
	$[H_4L](NO_3)_4$	
N2−H2B···N1n	2.816(1)	141.2(1)
N2−H2B···O2n	2.015(1)	160.4(1)
N3−H3B···O6n	2.142(1)	135.9(1)
N2−H2A···O4n#1	2.012(1)	143.3(1)
N2−H2A···N2n#1	2.883(1)	148.9(1)
N3−H3A···N4n#2	2.500(1)	171.5(1)
N3−H3A···O11n#2	2.298(1)	145.2(1)
N3−H3A···O12n#2	2.017(1)	155.2(1)
N5−H5B···N1n#2	2.667(1)	144.9(1)
N5−H5B···O3n_$2	2.118(1)	164.5(1)
N6−H6D···N3n#3	2.648(1)	152.6(1)
N6−H6D···O7n#3	2.275(1)	159.8(1)
	$[Cu_2LCl_2](NO_3)_2$ (**5**)	
N3−H3A···O1n	2.126(1)	144.7(2)
N2−H2A···O1n#4	2.091(1)	153.1(2)
	$[Cu_2L(NO_3)_2](NO_3)_2$ (**6**)	
N3−H1n···O5n	2.304(1)	140.7(4)
N2−H2n···N2n#5	2.829(1)	137.7(4)
N2−H2n···O5n#5	2.176(1)	161.3(4)
	$[Cu_2L(\mu\text{-}OH)](ClO_4)_3\cdot H_2O$ (**7**)	
N2−H2A···O11	2.308(1)	130.4(3)
N3−H3A···O8	2.274(1)	135.9(3)
N5−H5···O12	2.186(1)	156.1(4)
N6−H6···O5	2.504(1)	131.6(4)
O1p−H1p···O11	2.143(1)	155.3(7)
O1w−H2w···O10	2.388(1)	156.5(9)
O1w−H1w···O4#6	2.022(1)	168.0(8)

[a] #1, $-x+1, -y+1, -z$; #2, $x+1, +y, +z$; #3, $-x+2, -y, -z+1$; #4, $x+1, +y, +z$; #5, $x+1, +y, +z$; #6, $-x+2, -y, -z+1$.

Crystal Structures of ***6*** *and* ***7***. Crystals suitable for study by X-ray diffraction with the formulas $[Cu_2L(NO_3)_2](NO_3)_2$ (**6**) and $[Cu_2L(\mu\text{-}OH)](ClO_4)_3\cdot H_2O$ (**7**) were obtained by the slow evaporation of a water solution of the nitrate **3** and perchlorate **4** complexes with the ligand **L**, respectively.

The crystal structure of **6** is shown in Figure 3a, together with the selected bond lengths and angles. The complex shows two Cu^{II} ions located in the macrocyclic cavity in an environment similar to that described above for **5**, which are coordinated to a nitrogen atom from a pyridine ring, two amine nitrogen atoms, and one sulfur atom. The coordination sphere around each copper ion is completed by a monodentate nitrate ion. The geometry can be described as a slightly distorted square pyramid (τ = 0.003). The three nitrogen atoms and the sulfur atom form the square-plane base of the pyramid (rms 0.0851) with the Cu^{II} atoms 0.15 Å out of the plane, and the oxygen atom of the nitrate ion is occupying the apical position. The longest bond to the copper atom corresponds to the sulfur atom, 2.3656 Å, and the

dx.doi.org/10.1021/ic200287f |*Inorg. Chem.* 2011, 50, 5596–5604

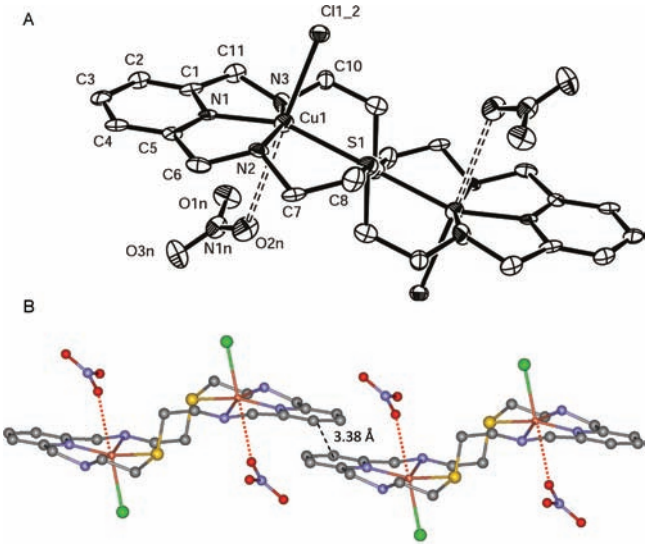

Figure 2. (a) Crystal structure of **5**. Selected bond lengths (Å) and angles (deg): Cu1−N1 1.940(7), Cu1−N2 2.027(8), Cu1−N3 2.077(8), Cu1−S1 2.374(3), Cu1−Cl1#1 2.506(3); N1−Cu1−N2 81.4(3), N1−Cu1−N3 80.8(3), N2−Cu1−N3 160.9(3), N1−Cu1−S1 158.7(2), N2−Cu1−S1 87.4(2), N3−Cu1−S1 107.2(2), N1−Cu1−Cl1#1 107.1(2), N2−Cu1−Cl1#1 96.4(2), N3−Cu1−Cl1#1 95.4(2), S1−Cu1−Cl1#1 92.00(9). Symmetry code: #1, $-x+1, -y+1, -z+1$. (b) π,π-Stacking interactions between the pyridine groups of adjacent molecules in **5**.

pyridinic nitrogen bond is again shorter (1.933 Å) than those of the amine groups (2.029 and 2.061 Å). The nitrate bond distance is 2.302 Å, and the Cu---Cu separation is 5.668 Å. If we take into account the long interaction established between a second nitrate and the metal ion (Cu1−O4n 2.692 Å), the coordination geometry could also be described as distorted octahedral.

The ligand shows a step conformation, with the planes containing the pyridine rings at 2.76 Å. Also, π,π-stacking interactions have been observed between the pyridine rings of adjacent molecules (Figure 3b). The distance between the planes containing these rings is 2.94 Å, and the distance between centroids is 3.53 Å. In the structure, there are a large number of hydrogen bonding interactions between the oxygen atoms of the nitrate groups and the free secondary amine groups of the ligand (see Table 2).

The crystal structures of **5** and **6** are similar to that previously described for $[Cu_2L'(NO_3)_4]$ and $[Cu_2L'(ClO_4)_4]$ complexes, where L′ is the related macrocycle Py_2N_6, with an amine group instead of the sulfur atom.[21] They also show a distorted octahedral environment around the Cu^{II} ions, but with one counterion at a longer bond distance than the other one, with the geometry being better described as a distorted square pyramid again. The shorter bond distances also correspond to the pyridinic nitrogen atoms, and the amine bond distance is similar to the values obtained here. The step conformation is also present in these complexes, although the pyridine rings are slightly farther than those reported here, but the overall disposition of the crystal lattice again shows π,π-stacking interactions.

The crystal structure of **7**, together with selected bond lengths and angles, is given in Figure 4. It shows two copper ions located inside the macrocyclic cavity joined by a hydroxyl bridge. The structure is similar to that found for $[Cu_2L(\mu\text{-OH})(CH_3NO_2)_2](BF_4)_3\cdot H_2O$.[12b]

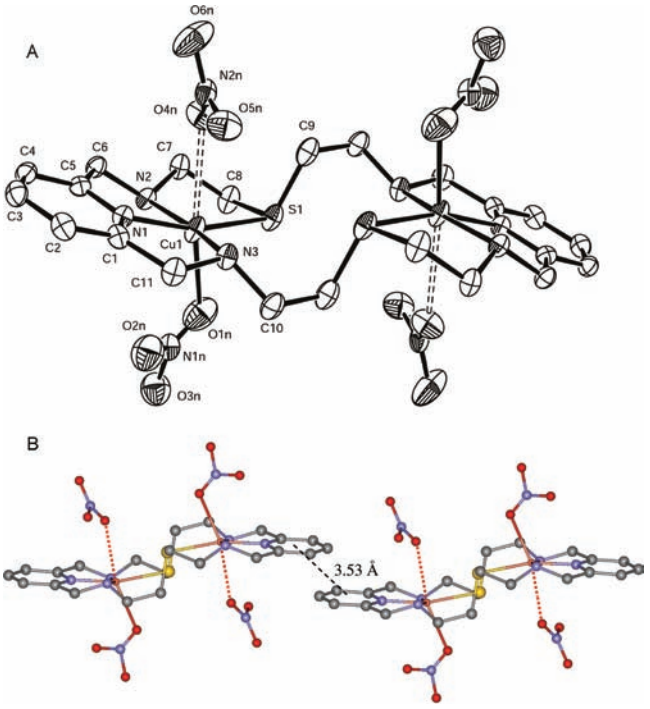

Figure 3. (a) Crystal structure of **6**. Selected bond lengths (Å) and angles (deg): Cu1−N1 1.933(3), Cu1−N2 2.029(3), Cu1−N3 2.061(3), Cu1−O1n 2.302(4), Cu1−S1 2.3656(11); N1−Cu1−N2 81.42(13), N1−Cu1−N3 82.17(13), N2−Cu1−N3 163.51(13), N1−Cu1−O1n 115.41(16), N2−Cu1− O1n 89.70(14), N3−Cu1−O1n 98.79(15), N1−Cu1−S1 163.35(10), N2−Cu1−S1 87.54(10), N3−Cu1−S1 108.10(10), O1n−Cu1−S1 76.72(13). (b) Crystal structure of **6** showing π,π-stacking interactions between the pyridine groups of adjacent molecules.

Each Cu^{II} atom is coordinated to one pyridinic nitrogen atom, two secondary amine nitrogen atoms, and one oxygen atom from a hydroxyl group acting as a bridge between the two metal centers. The rms values of the planes formed by the four atoms coordinated to each Cu^{II} ion are 0.0268 for Cu1 (plane N1−N2−N6−O1p) and 0.0633 for Cu2 (plane N3−N4−N5−O1p) with the metal atoms at 0.0457 Å (Cu1) and 0.0647 Å (Cu2) out of these planes. Therefore, the geometry can be best described as a slightly distorted square plane.

The hydroxyl group almost acts as a symmetric bridge between the copper ions and gives the shortest coordinated bond distances, 1.904 and 1.907 Å. The bond distances of the pyridinic rings, 1.933 and 1.932 Å, are shorter than the coordinated amine nitrogen atoms (2.075 Å, average value), and the Cu---Cu distance is 3.536 Å.

The dihedral angle between the planes containing the pyridine rings of the molecule is 47.71°, showing that the ligand is twisted. It is also folded because the angle between the pyridine nitrogen atoms and the oxygen atom of the −OH group acting as a bridge is 136.3°. The sulfur atoms are not coordinated, but they are oriented to the Cu^{II} ion at distances longer than those of the remaining coordinated atoms (Cu1−S1 2.815 Å and Cu2−S2 2.799 Å). In addition, one oxygen atom from a ClO_4^- group is oriented toward the Cu2 atom (Cu2−O1 2.814 Å), and the oxygen atom from the water molecule is located 2.666 Å from Cu1. Taking into account all of the weak interactions in the axial positions, the coordination geometry could also be considered as tetragonally distorted octahedral. In addition, the structure

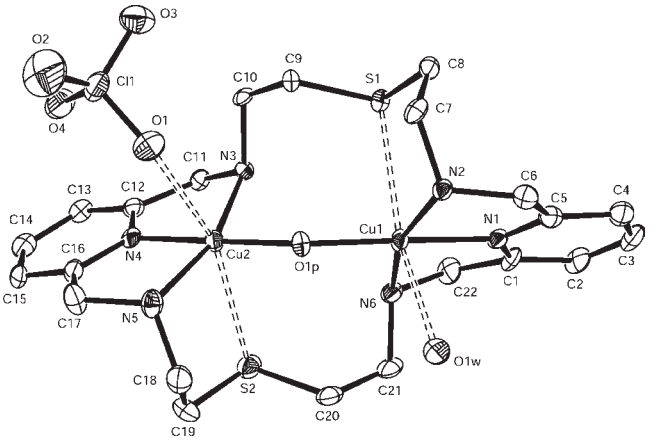

Figure 4. Crystal structure of **7**. Selected bond lengths (Å) and angles (deg): Cu1−O1p 1.904(4), Cu1−N1 1.933(5), Cu1−N2 2.069(5), Cu1−N6 2.099(5), Cu2−O1p 1.907(4), Cu2−N4 1.932(5), Cu2−N5 2.048(5),Cu2−N3 2.087(5), Cu1−S1 2.815(3), Cu2−S2 2.7987(19); O1p−Cu1−N1 178.81(19), O1p−Cu1−N2 98.0(2), N1−Cu1−N2 82.3(2), O1p−Cu1−N6 98.9(2), N1−Cu1−N6 80.7(2), N2−Cu1−N6 162.6(2), O1p−Cu2−N4 179.8(2), O1p−Cu2−N5 97.1(2), N4−Cu2−N5 83.0(2), O1p−Cu2−N3 98.83(19), N4−Cu2−N3 81.0(2), N5−Cu2−N3 162.5(2), O1p−Cu2−S2 89.29(14), N4−Cu2−S2 90.83(15), N5−Cu2−S2 83.45(16), N3−Cu2−S2 103.87(14), Cu1−O1p−Cu2 136.3(3).

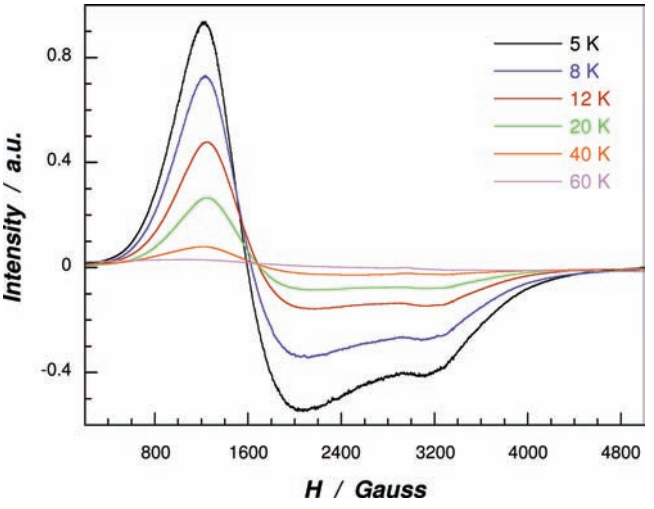

Figure 5. X-band EPR powder spectra of compound **1** recorded at different temperatures.

shows a large number of hydrogen-bond interactions between the perchlorate, the water molecule, and the free secondary amine groups of the ligand molecule (see Table 2).

EPR Spectroscopy. X-band electron spin resonance spectra of copper(II) nitrate and perchlorate complexes with **L**, **1**, and **2** were recorded as powdered samples from 4.2 to 300 K. At low temperatures, a very broad approximately reverse axial signal is observed for both complexes. The observed g values are $g_{\perp} = 5.25$ and $g_{\parallel} = 2.16$ for the nitrate compound **1** (Figure 5), whereas for the perchlorate complex **2**, only $g_{\perp}$ can be unambiguously determined and $g_{\perp} = 5.43$ because of the existence of a weak additional signal with unknown origin in the 3200 G region. Increasing the temperature to 100 K caused a further broadening of the

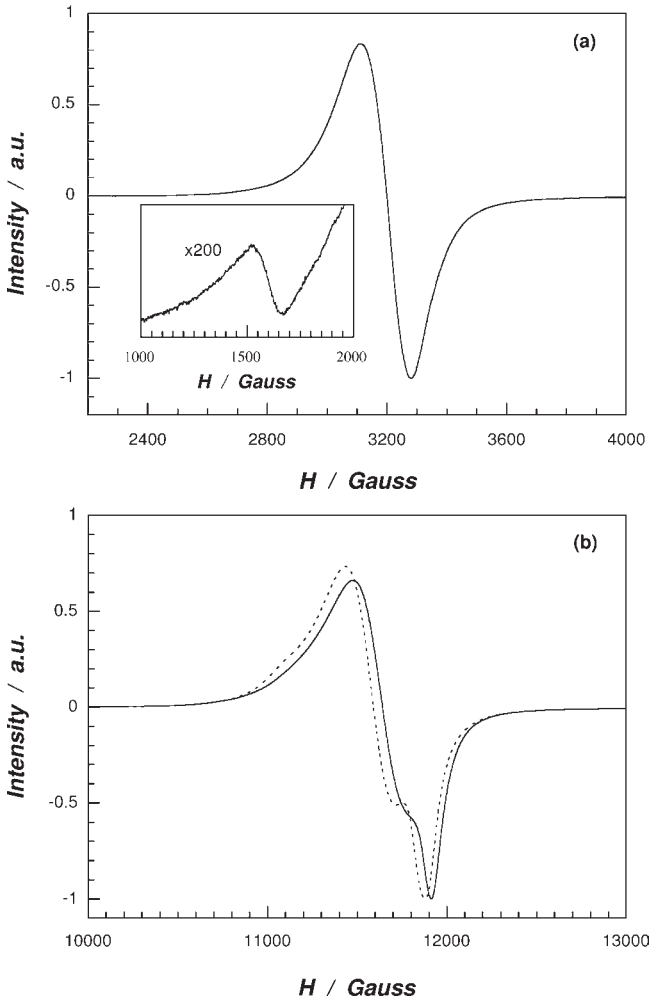

Figure 6. (a) X-band EPR powder spectrum of compound **3** at room temperature. (b) Q-band EPR spectra of compounds **3** (broken line) and **4** (full line) at room temperature.

bands, and above this temperature, the compounds became silent to EPR.

Both the strong anisotropy of the g factor and a very short spin−lattice relaxation time, which precludes observation of the EPR signals at room temperature, are usually found for Co^{II} ions in distorted octahedral sites. In fact, the observed spectra for both complexes can be described in terms of a spin doublet $S' = {}^1/_2$ that arises from the splitting of the $^4T_1$ term through spin−orbit coupling and local distortion of the octahedral sites.[22] The ^4F ground state of isolated Co^{II} in a purely octahedral crystal field splits into two orbital triplets, $^4T_1$ and $^4T_2$, and one orbital singlet, $^4A_2$. Spin−orbit effects and lower symmetry crystal fields produce further splitting of the $^4T_1$ triplet, giving a set of three levels: one doublet, one quartet, and one sextet, with the doublet being the low-lying state ($\lambda = -170$ cm^{-1} for the free ion). Notwithstanding, in most cases, it is found that the trace of the **g** tensor is close to the cubic isotropic value,[23,24] i.e., the three orthogonal g values are expected to be equal to in first order the value of 13 ($g_{iso} = 4.33$), as occurs for **1** ($\Sigma_g = 12.66$; $g_{av} = 4.22$). Moreover, because a quartet and a sextet are only a few hundred reciprocal centimeters above the ground state, fast electronic relaxation is commonly observed; hence, EPR spectra are only observed at low temperatures.[25]

dx.doi.org/10.1021/ic200287f |*Inorg. Chem.* 2011, 50, 5596–5604

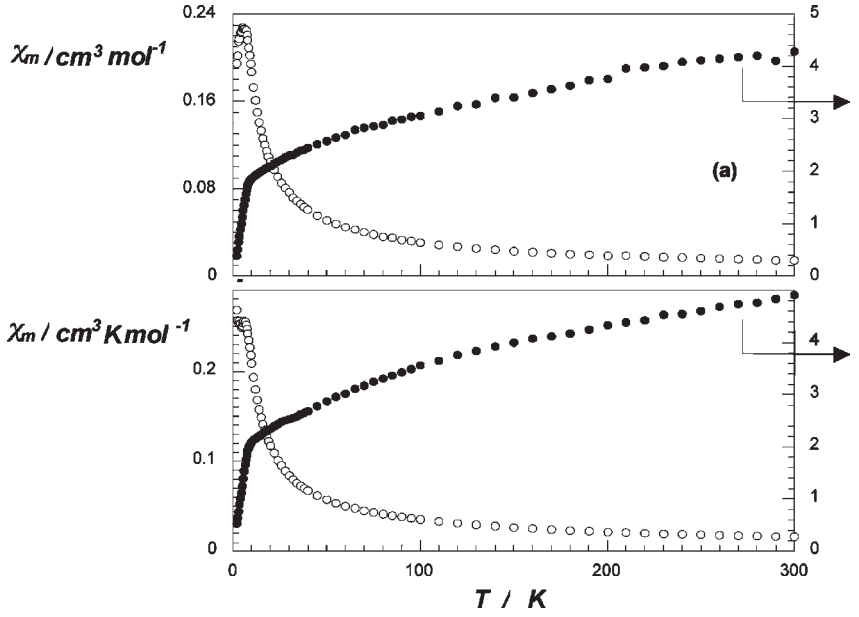

Figure 7. Thermal evolution of the χ_m ($cm^3\ mol^{-1}$) and $\chi_m T$ ($cm^3\ K\ mol^{-1}$) values for compounds **1** (a) and **2** (b).

EPR spectra of copper(II) complexes **3** and **4** were recorded as powdered samples between 4.2 and 300 K at both X and Q bands (Figure 6). The X-band spectra are not well-resolved because of a rather large linewidth, and quasi-isotropic signals are observed. However, at the Q band the signals are clearly characteristics of rhombic **g** tensors with the following main values: $g_1 = 2.180$, $g_2 = 2.107$, and $g_3 = 2.052$ ($g_{av} = 2.113$) for the nitrate complex and $g_1 = 2.165$, $g_2 = 2.101$, and $g_3 = 2.047$ ($g_{av} = 2.104$) for the perchlorate complex. In the X-band spectra of both compounds, besides the large signal mentioned above, which corresponds to the $\Delta M_s = \pm 1$ allowed transitions, a weak feature around 1600 G is also observed. This second signal is attributable to $\Delta M_s = \pm 2$ forbidden transitions and agrees with the existence of a triplet state and therefore a dimeric structure according to the chemical formulas. Notwithstanding, the low intensity of this signal and the absence of a hyperfine structure suggest the presence of some type of extended magnetic exchange, probably via hydrogen bonding. In any case, the intra- and/or interdimeric exchange must necessarily be weak considering that the spectra remain unchanged when cooling down to 4.2 K.

The significant deviation of the lowest *g* from the free electron value (2.0023) is indicative of a $d_{x^2-y^2}$ ground state for the copper(II) chromophores, and it is compatible with square-pyramidal or tetragonally elongated octahedral geometries.[26] Moreover, the relatively low values of the g_1 components suggest the presence of weakly bonded axial ligands. However, this last hypothesis must be considered with caution because of the possible existence of magnetic interactions between magnetically nonequivalent Cu^{II} ions. If such interactions are present, the experimental *g* values are not equal to the molecular ones and therefore they do not necessarily reflect the topology of the copper arrangement. The *g* values obtained from the experiment can be tested to decide if they are actually molecular by the parameter *G*:

$$G = (g_1 - g_2)/[g_2 + g_3)/2 - g_0] \qquad (1)$$

where g_0 is the free electron value $g = 2.0023$. The obtained *G* parameters are about 2.3 for both complexes, indicating that magnetic interactions between nonparallel chromophores in the compounds cause experimental *g* values that do not correspond to the molecular ones. This misalignment is probably the origin of the quasi-isotropic lines observed working at an X band.

Magnetic Studies. The magnetic susceptibility for **1** and **2** was measured from 1.8 to 300 K. The resulting plots of χ_m vs *T* and $\chi_m T$ vs *T* are given in Figure 7. For **1**, the susceptibility increases with decreasing temperature, reaching its maximum value at about 5.5 K, and decreases until 1.8 K. For **2**, behavior basically similar to that of $T_{max} = 6$ K is observed, but with a further increase of the susceptibility below 4 K. The high-temperature data ($T > 100$ K) obey the Curie−Weiss law with large and negative Weiss constants of $\theta = -85.7$ and -75.4 K and Curie constant (C_m) values of 5.47 and 6.08 $cm^3\ K\ mol^{-1}$ for **1** and **2**, respectively. The room temperature values of the effective magnetic moment, $\mu_{eff} = (8\chi_m T)^{1/2}$, are 5.86 and 6.25 μ_B for the nitrate and perchlorate compounds, respectively, which are in good agreement with those observed for Co^{II} ions in distorted octahedral arrangements and allow us to assign an effective spin of $S = {}^3/_2$ for both complexes at room temperature. The magnetic moments slowly decrease from 300 to 15 K and more rapidly at lower temperatures.

The above-described magnetic behaviors are consistent with the existence of antiferromagnetic interactions between the Co^{II} ions. However, the effect of the spin−orbit coupling on octahedral cobalt(II) compounds should also be taken into consideration. Thus, while at high temperatures the excited states are usually occupied and an $S = {}^3/_2$ configuration, with an important orbital contribution, is obtained, at low temperatures, only the ground state is thermally accessible, and although it is a spin−orbit doublet, the situation may be characterized by an effective spin $S' = {}^1/_2$. This is consistent with the observed EPR spectra and obviously affects the magnetic susceptibility measurements. Actually, this phenomenon causes an effect qualitatively similar to that originating from the antiferromagnetic interactions, and it becomes difficult to distinguish between these two contributions when they have comparable values. Considering the large values of the

dx.doi.org/10.1021/ic200287f |*Inorg. Chem.* 2011, 50, 5596–5604

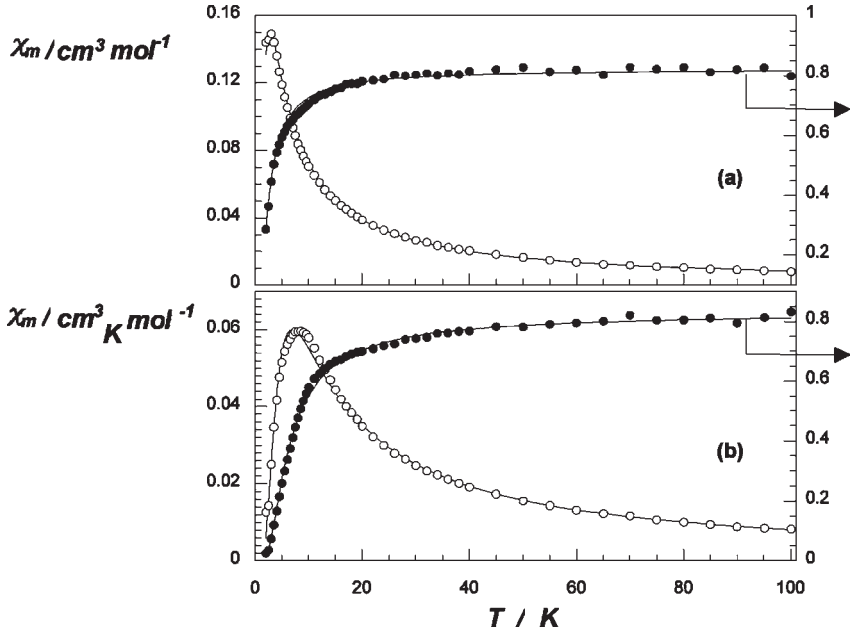

Figure 8. Thermal evolution of the χ_m ($cm^3\ mol^{-1}$) and $\chi_m T$ ($cm^3\ K\ mol^{-1}$) values for compounds **3** (a) and **4** (b). Full lines represent the theoretical values for dimeric systems (see the text).

Weiss constants compared to the low T_{max} temperatures, it can be concluded that both contributions should be simultaneously considered in both complexes.

Variable-temperature magnetic susceptibility measurements were also performed as powdered samples of copper compounds **3** and **4** in the 1.8−300 K range. The thermal evolution of both the magnetic molar susceptibility and $\chi_m T$ values is shown in Figure 8 (only the data below 100 K have been represented). In both cases, the susceptibility increases with decreasing temperature, reaching a maximum, after which it rapidly decreases. The maxima are located at 3 and 7.5 K, for **3** and **4**, respectively. The Curie−Weiss law is only followed in the high-temperature range ($T > 20$ K), for which values of C_m = 0.83 (**3**) and 0.85 $cm^3\ K\ mol^{-1}$ (**4**) and $\theta = -1.3$ (**3**) and −3.2 K (**4**) have been calculated. The observed Curie constants agree quite well with those calculated using the g values obtained from the EPR data. The negative θ values, together with the continuous decrease of the effective magnetic moments observed when the temperature is lowered, are indicative of the predominance of antiferromagnetic interactions in these compounds. Moreover, the observed magnetic behavior appears to correspond to systems with prevailing short-range interactions: the susceptibility tends to zero with the temperature, and the decrease of the effective magnetic moment is very fast below 20 K. This fact is consistent with the dimeric structure that can be proposed for both compounds after the chemical formula and the EPR results.

Considering only dimeric couplings, one can easily estimate the exchange parameter J between Cu^{II} ions from the temperature at which the susceptibility reaches the maximum value [$T(\chi_{max}) = 1.25|J|/k$], as well as from the Weiss temperature ($\theta = J/2k$). The calculated J/k values are about 2.5 and 6 K for the copper nitrate and perchlorate compounds, respectively. A more complete description of the observed magnetic behaviors may be obtained by using the Bleaney−Bowers equation of copper dimers,[27] derived from the Heisenberg spin Hamiltonian ($H = -2JS_1S_2$) for two coupled $S = {}^1/_2$ ions:

$$\chi_m = (2Ng^2\beta^2/kT)[3 + \exp(-2J/kT)]^{-1} \qquad (2)$$

where N is Avogadro's number, β the Bohr magneton, and k Boltzmann's constant. The best least-squares fits (solid lines in Figure 8) were obtained for the exchange parameters $J/k = -2.2$ and -5.6 K with $g = 2.10$ and 2.11 for **3** and **4**, respectively. The good agreement between experimental and calculated data confirm the dimeric structure suggested for these compounds. The observed small J values imply a poor overlap between the magnetic orbitals (mainly $d_{x^2-y^2}$) of the two Cu^{II} ions.

CONCLUSIONS

In summary, the work presented here describes the synthesis and characterization of new cobalt(II) and copper(II) dinuclear nitrate and perchlorate complexes with the $Py_2N_4S_2$-coordinating octadentate macrocyclic ligand (**L**) and its protonated form, $[\mathbf{H_4L}]\mathbf{Cl_4}$. The crystal structure of the protonated ligand $[H_4L]^{4+}$ shows two different conformations, planar and step, and the existence of intermolecular face-to-face π,π-stacking interactions between the pyridinic rings, giving rise to infinite chains. The crystal structures of **5** and **6** have the metal ions in a slightly distorted square-pyramidal geometry. In the case of **7**, the crystal structure presents the two metal ions joined by a μ-hydroxo bridge and the Cu^{II} centers in a slightly distorted square-planar geometry. The structures could also be considered as distorted octahedral if we take into account weak interactions. The EPR spectroscopy and magnetic studies agree with the dinuclear nature for the complexes, with an octahedral environment for cobalt(II) and square-pyramidal or tetragonally elongated octahedral geometries for copper(II) compounds. The magnetic behavior is consistent with the existence of antiferromagnetic interactions between the ions for all complexes.

dx.doi.org/10.1021/ic200287f |*Inorg. Chem.* 2011, 50, 5596–5604

Crystallographic data have been deposited as CCDC 742725−742728 for $[H_4L](NO_3)_4$, $[Cu_2LCl_2](NO_3)_2$ (**5**), $[Cu_2L(NO_3)_2](NO_3)_2$ (**6**), and $[Cu_2L(\mu\text{-}OH)](ClO_4)_3\cdot H_2O$ (**7**), respectively. These data can be obtained free of charge at www.ccdc.cam.uk/conts/retrieving.html [or from the Cambridge Crystallographic Data Centre, 12 Union Road, Cambridge CB2 1EZ, U.K.; fax (international) +44-1223/336-033; e-mail deposit@ccdc.cam.ac.uk].

AUTHOR INFORMATION

Corresponding Author

*E-mail: mrufina.bastida@usc.es (R.B.), qilaura@uvigo.es (L.V.).

ACKNOWLEDGMENT

We thank the Xunta de Galicia (Spain; Projects 10PXIB20-9028PR and INCITE09E1R209058ES) for financial support. L.V. thanks the Xunta de Galicia for the *Isidro Parga Pondal* Research program. R.B. thanks the Xunta de Galicia for the research stay grant at the Universidad del País Vasco. C.N. is thankful the Fundação para a Ciência e a Tecnologia/FEDER (Portugal/EU) programme postdoctoral contract (SFRH/BPD/65367/2009).

REFERENCES

(1) (a) Latour, J. M. *Bull. Soc. Chim. Fr.* **1988**, 508. (b) Sorrell, T. N. *Tetrahedron* **1989**, *45*, 3. (c) Vigato, P. A.; Tamburini, S.; Fenton, D. *Coord. Chem. Rev.* **1990**, *106*, 25. (d) Kitajima, N. *Adv. Inorg. Chem.* **1992**, *39*, 1. (e) Karlin, K. D.; Tyekler, Z. *Bioinorganic Chemistry of Copper*; Chapman and Hill: New York, 1993. (f) Holz, R. C.; Brink, J. M.; Gobena, F. T.; O'Connor, C. J. *Inorg. Chem.* **1994**, *33*, 6086. (g) Holz, R. C.; Bradshaw, J. M.; Bennet, B. *Inorg. Chem.* **1998**, *37*, 1219.

(2) (a) Neves, A.; Rossi, L. M.; Vencato, I.; Drago, V.; Hasse, W.; Werner, R. *Inorg. Chim. Acta* **1998**, *281*, 111. (b) Torelli, S.; Belle, C.; Gautier-Luneau, I.; Pierre, J. L.; Saint-Aman, E.; Latour, J. M.; LePape, L.; Luneau, D. *Inorg. Chem.* **2000**, *39*, 3526. (c) Neves, A.; Rossi, L. M.; Bortoluzzi, A. J.; Mangrich, A. S.; Hasse, W.; Werner, R. *J. Braz. Chem. Soc.* **2001**, *12*, 747. (d) Dapporto, P.; Formica, M.; Fusi, V.; Giorgi, L.; Micheloni, M.; Paoli, P.; Pontellini, R.; Rossi, P. *Inorg. Chem.* **2001**, *40*, 6186. (e) Fondo, M.; García-Deibe, A. M.; Sanmartin, J.; Bermejo, M. R.; Lezama, L.; Rojo, T. *Eur. J. Inorg. Chem.* **2003**, 3703.

(3) (a) Peralta, R. A.; Neves, A.; Bortoluzzi, A. J.; dos Anjos, A.; Xavier, F. R.; Szpoganicz, B.; Terenzi, H.; de Oliveira, M. C. B.; Castellano, E.; Friedermann, G. R. D.; Mangrich, A. S.; Novak, M. A. *J. Inorg. Biochem.* **2006**, *100*, 992. (b) Weng, C. H.; Cheng, S. C.; Wei, H. H.; Lee, C. J. *Inorg. Chim. Acta* **2006**, *359*, 2029. (c) Rey, N. A.; Neves, A.; Bortoluzzi, A. J.; Pich, C. T.; Terenz, H. *Inorg. Chem.* **2007**, *46*, 348. (d) Ackermann, J.; Buchler, S.; Meyer, F. *C. R. Chim.* **2007**, *10*, 421.

(4) Linder, M. C.; Goode, C. A. *Biochemistry of Copper*; Plenum: New York, 1991.

(5) Solomon, E. I.; Baldwin, M. J.; Lowery, M. D. *Chem. Rev.* **1992**, *92*, 521.

(6) Solomon, E. I.; Sundaram, U. M.; Machonkin, T. E. *Chem. Rev.* **1996**, *96*, 2563.

(7) Magnus, K. A.; Ton-That, H.; Carpenter, J. E. *Chem. Rev.* **1994**, *94*, 727.

(8) Klabunde, T.; Eicken, C.; Sacchettini, J.; Krebs, B. *Nat. Struct. Biol.* **1998**, *5*, 1084.

(9) Kobayashi, M.; Shimizu, S. *Eur. J. Biochem.* **1999**, *261*, 1.

(10) (a) Adrait, A.; Jacquamet, L.; Le Pape, L.; Gonzalez de Peredo, A.; Aberdam, D.; Hazemann, J. L.; Latour, J. M.; Michaud-Soret, I. *Biochemistry* **1999**, *38*, 6248. (b) Strand, K.; Karlsen, S.; Andersson, K. K. *J. Biol. Chem.* **2002**, *277*, 34229.

(11) Lindoya, L. F.; Meehan, G. V.; Vasilescu, I. M.; Kim, H. J.; Lee, J.-E.; Lee, S. S. *Coord. Chem. Rev.* **2010**, *254*, 1713.

(12) Núñez, C.; Bastida, R.; Macías, A.; Valencia, L.; Ribas, J.; Capelo, J. L.; Lodeiro, C. *Dalton Trans.* **2010**, *39*, 7673. (b) Núñez, C.; Bastida, R.; Macías, A.; Valencia, L.; Neuman, N. I.; Rizzi, A. C.; Brondino, C. D.; González, P. J.; Capelo, J. L.; Lodeiro, C. *Dalton Trans.* **2010**, *39*, 11654.

(13) Steenland, M. W. A.; Lippens, W.; Herman, G. G.; Goeminne, A. M. *Bull. Soc. Chim. Belg.* **1993**, *102*, 239.

(14) Sheldrick, G. M. *SADABS, Program for Empirical Absorption Correction of Area Detector Data*; University of Göttingen: Göttingen, Germany, 1996.

(15) *SHELXTL version, An Integrated System for Solving and Refining Crystal Structures from Diffraction Data*, revision 5.1; Bruker AXS Ltd: Madison, WI, 1997.

(16) Farrugia, L. J. *J. Appl. Crystallogr.* **1997**, *30*, 565.

(17) (a) Grill, N. S.; Nuttall, R. H.; Scaife, D. E.; Sharp, D. W. J. *Inorg. Nucl. Chem.* **1961**, *18*, 79. (b) Aime, S.; Botta, M.; Casellato, U.; Tamburini, S.; Vigato, P. A. *Inorg. Chem.* **1995**, *34*, 5825.

(18) Guerriero, P.; Casellato, U.; Tamburini, S.; Vigato, P. A.; Graziani, R. *Inorg. Chim. Acta* **1987**, *129*, 127.

(19) Rosenthal, M. F. *J. Chem. Educ.* **1973**, *50*, 331.

(20) Geary, J. W. *Coord. Chem. Rev.* **1971**, *7*, 81.

(21) Martínez-Sánchez, J. M.; Bastida, R.; Macías, A.; Pérez-Lourido, P.; Valencia Matarranz, L. *Polyhedron* **2006**, *25*, 3495.

(22) Carlin, R. L. *Magnetochemistry*; Springer: Berlin, 1986.

(23) Abragam, A.; Pryce, M. H. L. *Proc. R. Soc. London, Ser. A* **1951**, *206*, 173.

(24) Abragam, A.; Bleaney, B. *EPR of Transition Ions*; Clarendon: Oxford, U.K., 1970.

(25) Weil, J. A.; Bolton, J. R.; Wertz, E. *Electron Spin Resonance, Elementary Theory and Practical Applications*, 2nd ed.; Wiley: New York, 1994.

(26) Hathaway, B. J.; Billing, D. E. *Coord. Chem. Rev.* **1970**, *5*, 143.

(27) Bleaney, B.; Bowers, K. D. *Proc. R. Soc. London, Ser. A* **1952**, *214*, 451.